2017 Floods in China

Measuring flood water extent and impact before and after flooding event using supervised classification

Research Question:

This research will use supervised land cover classification to determine the total flooded area based on observations taken from multispectral images of the study area before and after a major flooding event in Nanchang, Jiangxi, China.

Extensive flooding of the Yangtze River and Po Yang Lake due to heavy rains in late June, 2017 covered a huge swath of the surrounding areas even two weeks after the storm.

A comparison of supervised classification results from images before and after the storm could provide: classified images based on training data, and percent change in land cover type between the two images.

Background

Flooding has long been a catastrophic problem for human settlements, and has become more dangerous with the influence of global warming on precipitation trends in certain areas, and the drive towards increased urban development (Nirupama & Simonovic, 2002; Schumann et al. 2009).

The cost of flooding over time has been dramatic both in terms of human life and economic damages, and is expected to increase to over $52 billion dollars annually by the year 2050 (Hallegatte et al. 2013).

Background

Research into flood dynamics and disaster management practices have leveraged remote sensing to:

- develop hydraulic models for flood predictions (Bales et al. 2007; Myrland, 2014; Schumann et al. 2009)
- monitor flood extent and depth during floods (Haq et al. 2012; Rahman & Thakur, 2017)
- conduct damage assessments (Joyce et al. 2010; Womble et al. 2006)
- and aid search and rescue operations (Joyce et al. 2010).

These projects have relied on a variety of different platforms and sensors from high-resolution photography, radar and laser altimeters, SAR, Multispectral sensors (Alsdorf et al. 2005; Mason et al. 2014; Schumann, 2017; Womble et al. 2006), and even volunteered geographic information, or VGI (Poser, 2010).

Background

Water has a unique spectral signature in multispectral images as it absorbs — rather than reflects — much of the radiation measured by multispectral sensors. Consequently, areas that become more moist as a result of flooding or heavy rains have different spectral signatures compared to the same surfaces under dry conditions.

Band transformations like NDWI (McFeeters, 2013) — the normalized difference of the near-infrared and green bands — and NDVI (Womble et al. 2006) — the normalized difference of near-infrared and red bands — can also be used to isolate water area from other features.

If areas become completely inundated, classifiers will easily be able to detect the difference between flood waters and pre-flood conditions. Subtracting multitemporal rasters would indicate the difference in flood extent between images, and subtracting total area of each land cover class across the two images would demonstrate how flooding impacted certain types of land cover.

Examples of Flood Monitoring using RS

Clockwise from top left: TOF Lidar unit position along the Amacuzac River in Mexico; TrueSense S200 TOF Lidar, 64° incidence angle; Dispersion of laser light (indicated by the yellow arrow) in the water due to the Tyndall Effect; Researcher using a Secchi disk to assess turbidity (Tamari & Guerrero-Meza, 2016).

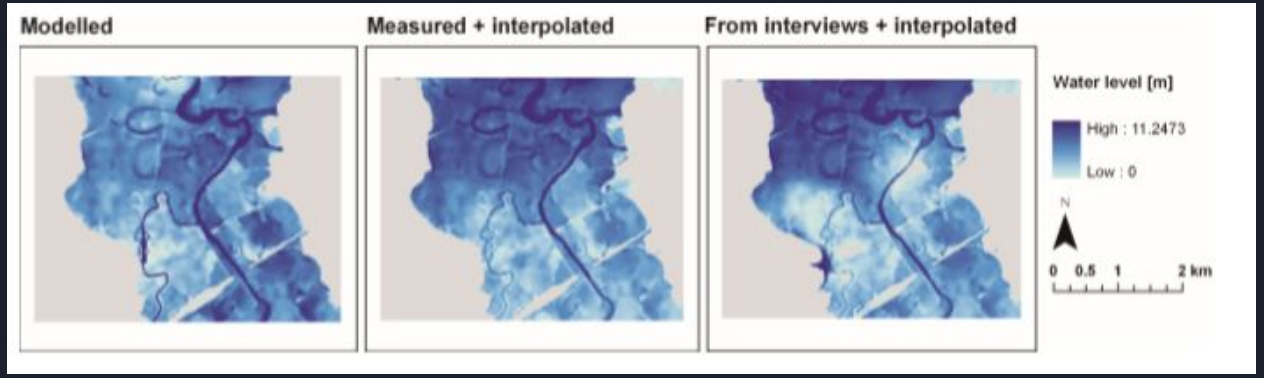

Modelled vs Interpolated flood depth surfaces in Eilenburg, Germany based on volunteered geographic information (Poser, 2010).

From left to right: Lidar image of an isolated building, double backscatter from TerraSAR-X in flooded conditions, and under normal conditions (Mason et al. 2014).

Supervised Classification for Flood Assessment:

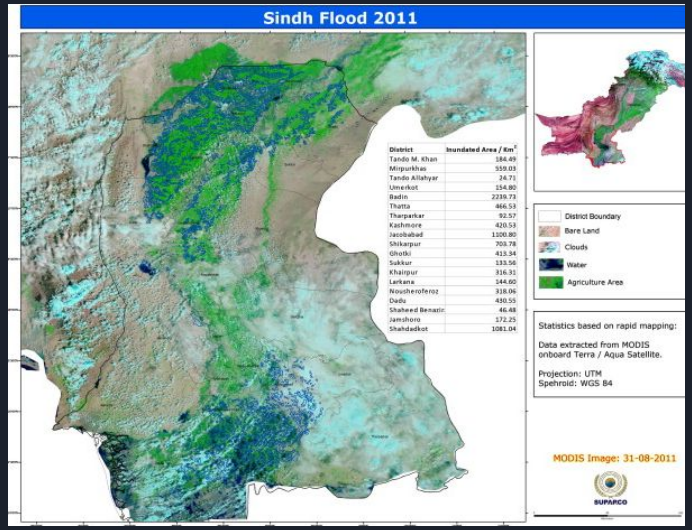

Classified MODIS imagery of flood area in Sindh, Pakistan. The inset chart displays flood areal extent summarized by district in (Haq et al. 2012).

NDVI differenced images after masking of New Orleans. Higher standard deviations in NDVI indicate greater impact of flooding (Womble et al. 2006).

Study Area and Data

In the summer of 2017, China experienced sustained rainfall that led to catastrophic flooding in many provinces throughout the country. This study focuses on the area around Nanchang and Po Yang Lake in Jiangxi, China.

Residential area in Nanchang, the capital city of Jiangxi Province China, June 22, 2017. Credit: Xinhuanet News

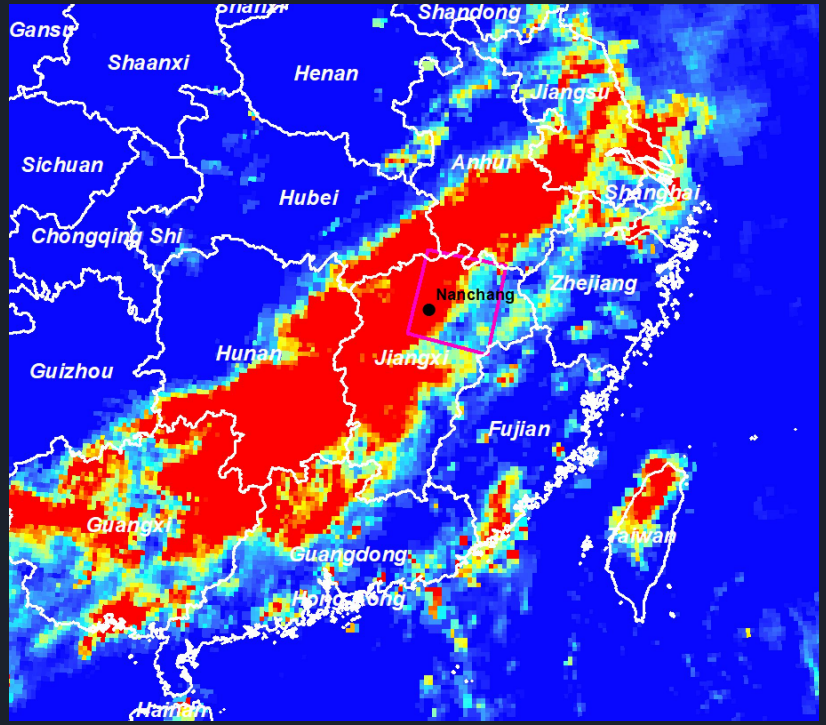

IMERG precipitation data from NASA GES DISC data service for July 1, 2017.

Study Area and Data

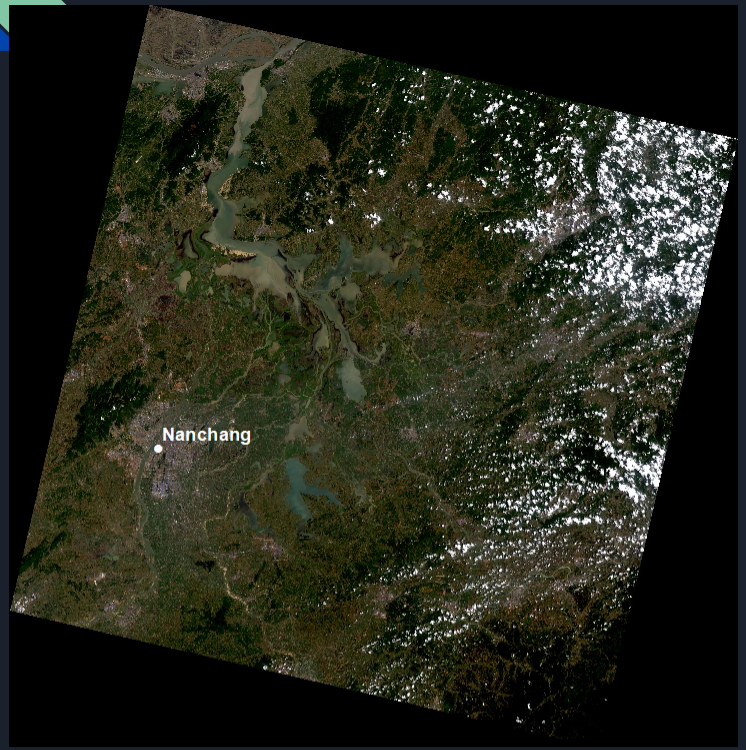

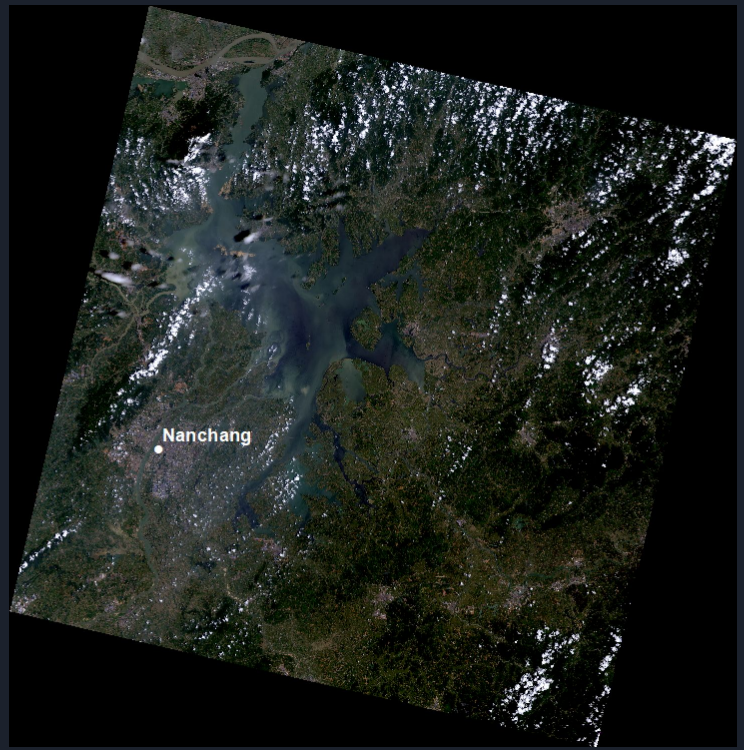

Multispectral Landsat 8 images of the study area from before and after storm (Path 121, Row 40) collected from USGS earth explorer.
Left: *May 9th, 2017*; **Right**: *July 12, 2017*

Process Overview

1. Preprocessing: Develop cloud masks to eliminate the influence of cloud cover and shadow on supervised classification
2. Qualitative analysis using different band combinations and NDVI
3. Design training dataset for classification in 5 classes: water (flood area), developed, agricultural, forest, and wetlands
4. Generate two classified images for before and after the storm
5. Conduct accuracy assessment

Preprocessing/Masking

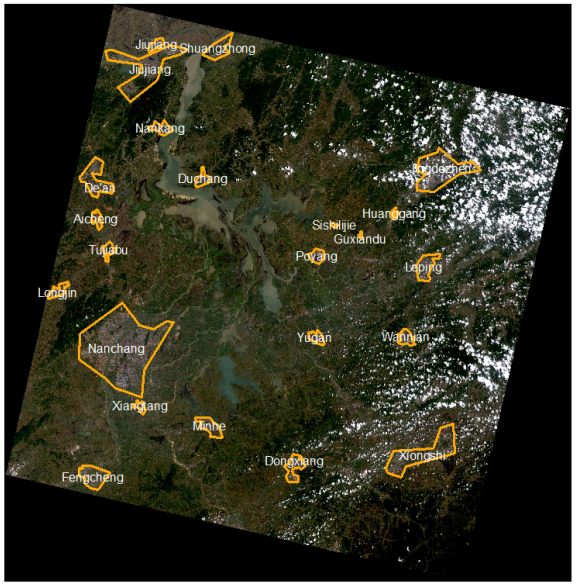

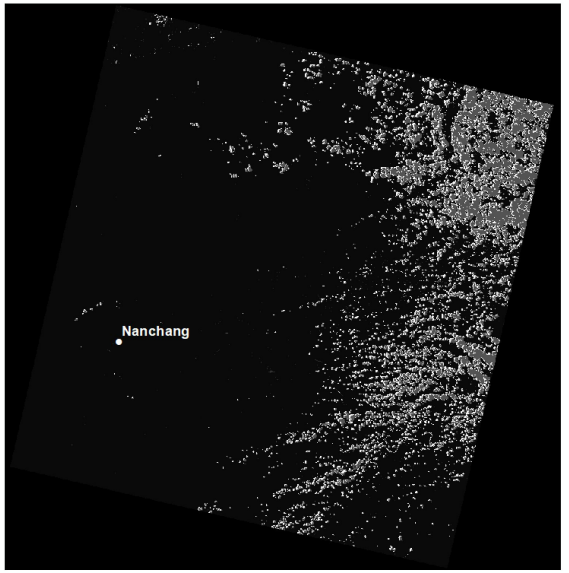

Left: *Landsat 8 OLI True Color Composite Image of Jiangxi, China (Path 121, Row 40) with populated areas.*
Right: *Same Location as Left, Landsat 8 Quality Assessment Band, which is a raster which shows bad pixels that may compromise a raster's scientific use. The QA bands were used to mask clouds and shadows caused by cloud cover.*

Preprocessing/Masking

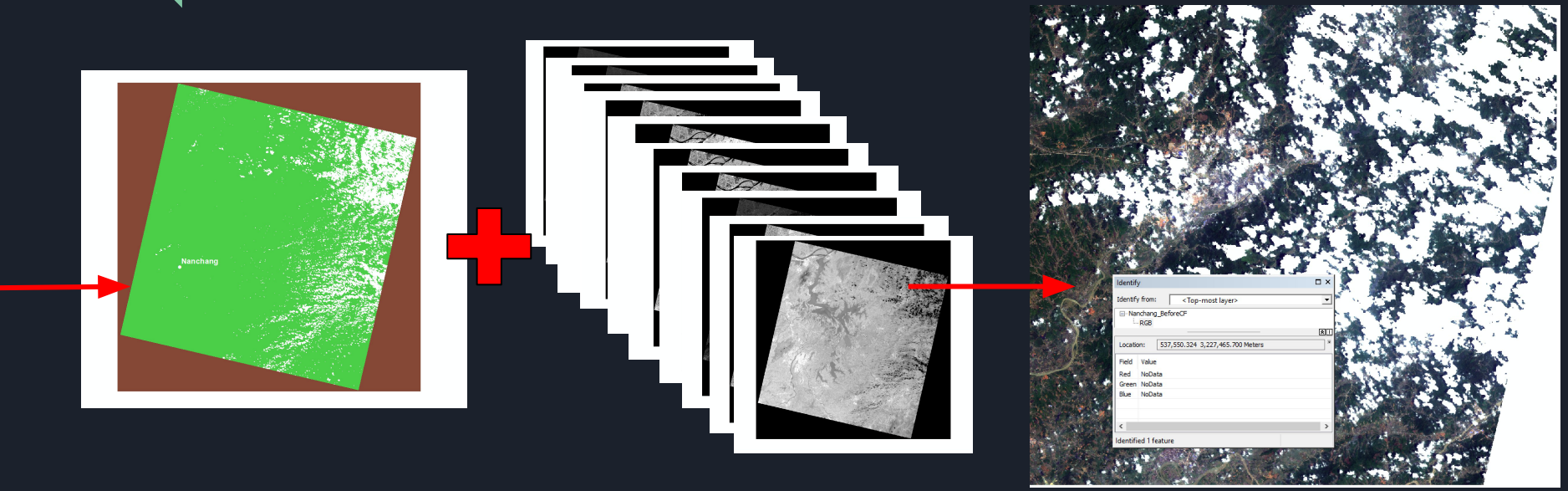

Above: *Use the reclassified cloud raster as an input to* [Raster Calculator] *formula* [cloudmaskraster * Band X], *for each of* X *images. This will turn preserve all data in each image but convert cloud cover to NoData. Then, use* [Composite Bands] *tool to join the individual cloud free images.*

Qualitative Analysis

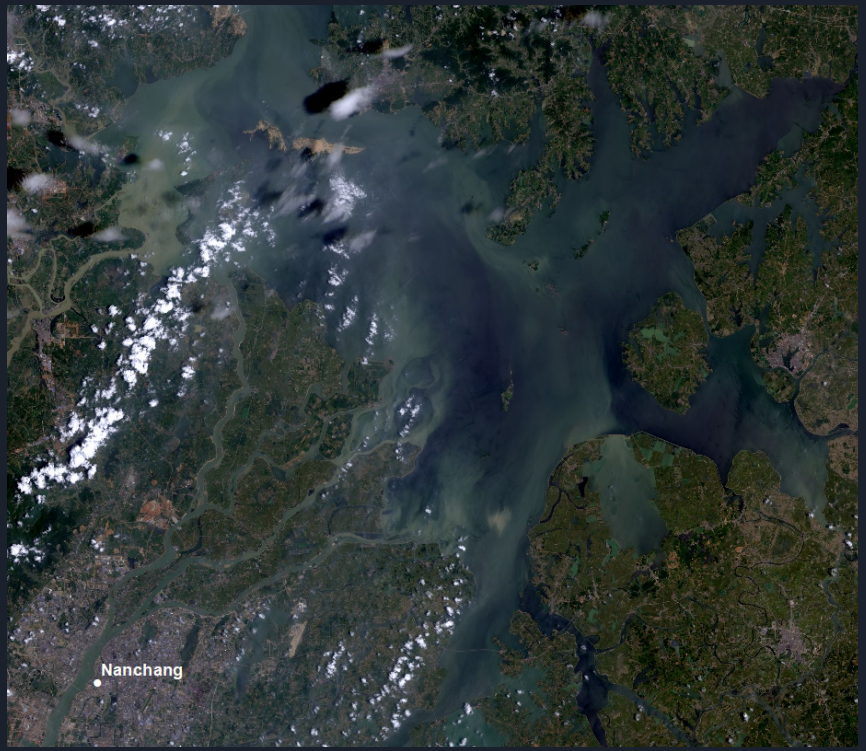

Left: *Before image shows lush wetlands between Nanchang city and agricultural area north of the city.* **Right**: *After image shows dramatic flooding, dilated rivers and complete inundation of wetland area.*

Qualitative Analysis

Left: *Before NIR, Red, Green false color composite image of a northern section of Nanchang,* **Right:** *dilated streams and surge line, as well as inundated river islands are evident in the image.*

Qualitative Analysis

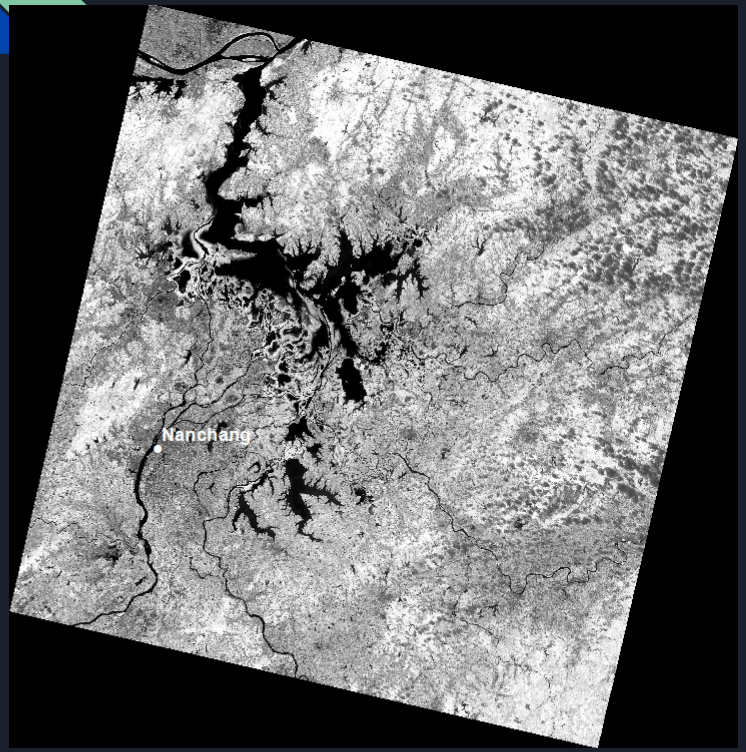

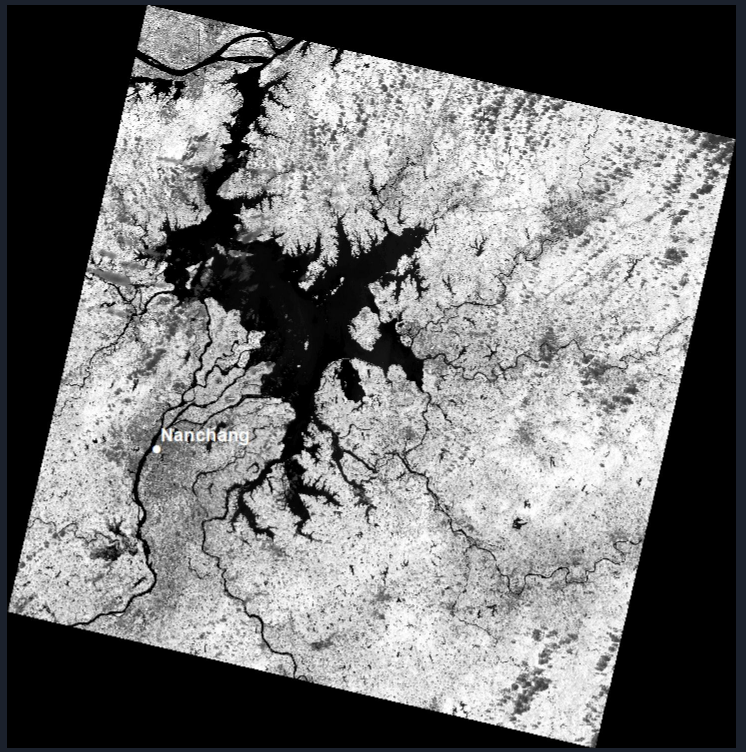

Grayscale NDVI images of the area show a dramatic change in inundated area. Po Yang Lake covers a much larger area and connects to some of the smaller lakes east of Nanchang. Smaller rivers and streams to the east of the lake are much more visible after the flood.

Supervised Classification Training Data

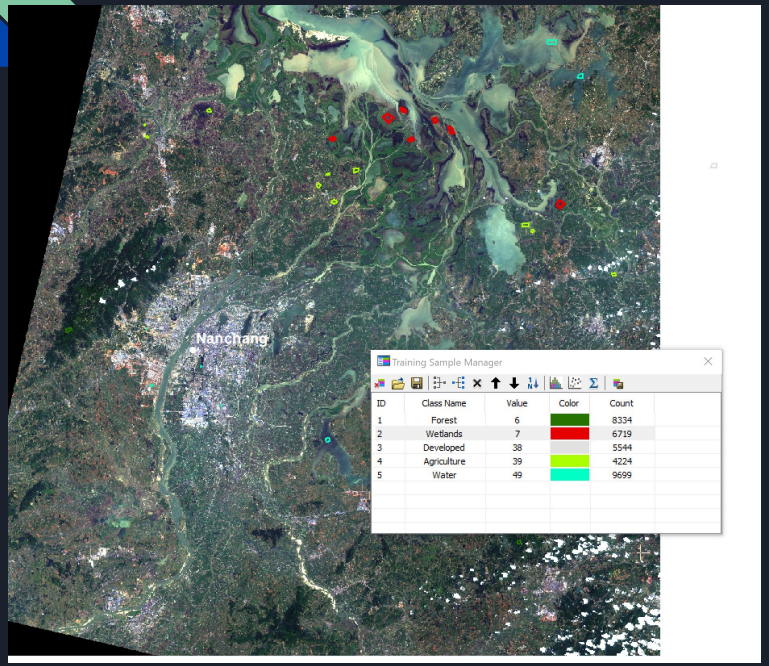

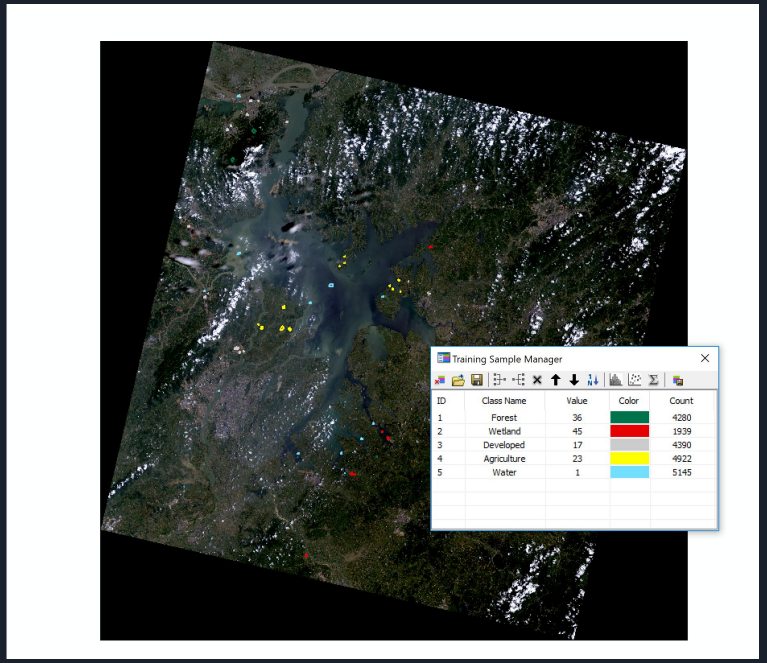

Generated two separate training sets for the before and after images to accommodate the shifting landscape. Forest, Wetlands, Developed, Agriculture, and Water

Supervised Classification Results

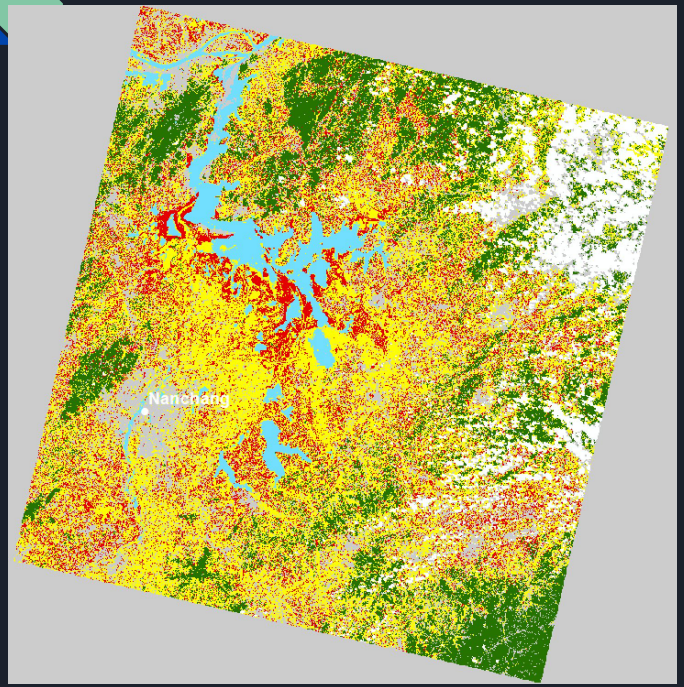

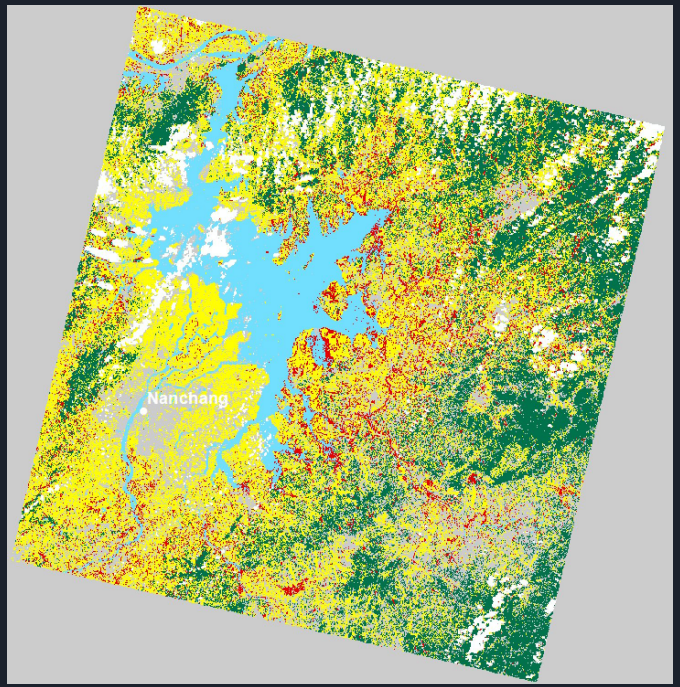

The result of the Interactive Supervised Classification. **Left**: *Before image*, **Right**: *After image. The difference in water area extent is immediately apparent and the classifier was able to effectively illustrate the destruction of the wetlands area south of Po Yang Lake.*

Supervised Classification Results

	PreFlood	PostFlood	% Change
Forest	6731670	8396996	124.74
Wetlands	5509368	2494161	45.27
Developed	26172042	27640804	105.61
Agriculture	14347360	12834170	89.45
Water	1939610	4015581	207.03

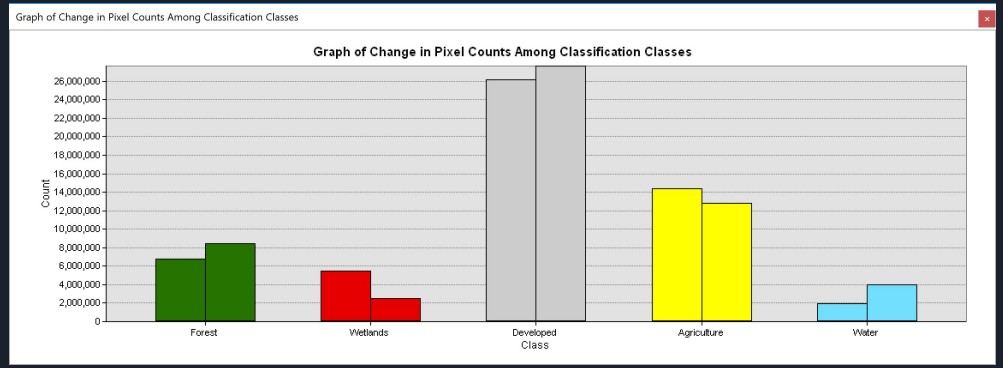

Used [Cell Statistics] *to calculate the count of cells in each class and then calculated percent change and charted the results. Some of the classes were a bit confused because of the nature of the scene and imperfect training data, but the dramatic change in wetlands (45%) and water (207%) classes was due to flood extent increase. During the qualitative analysis it was apparent that agricultural land also was impacted by the change in water extent.*

Accuracy Assessment/Confusion Matrix

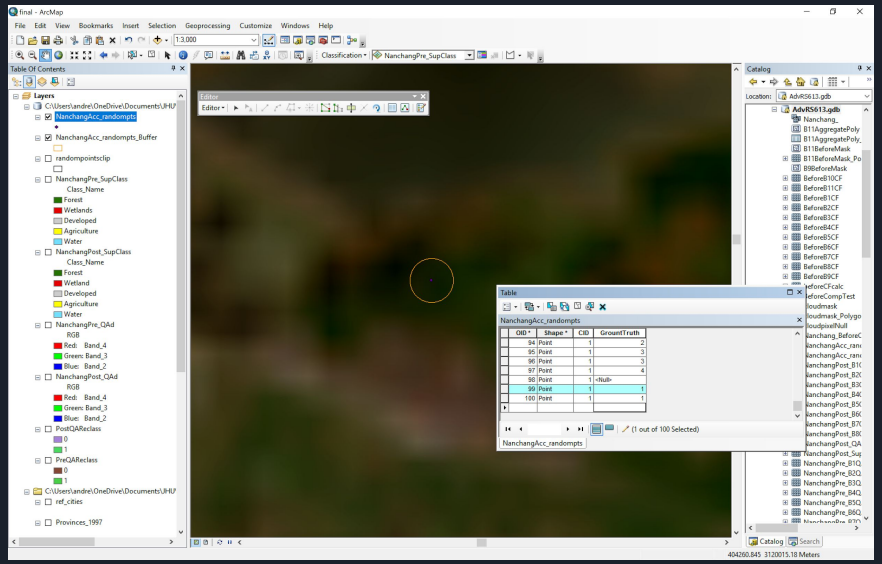

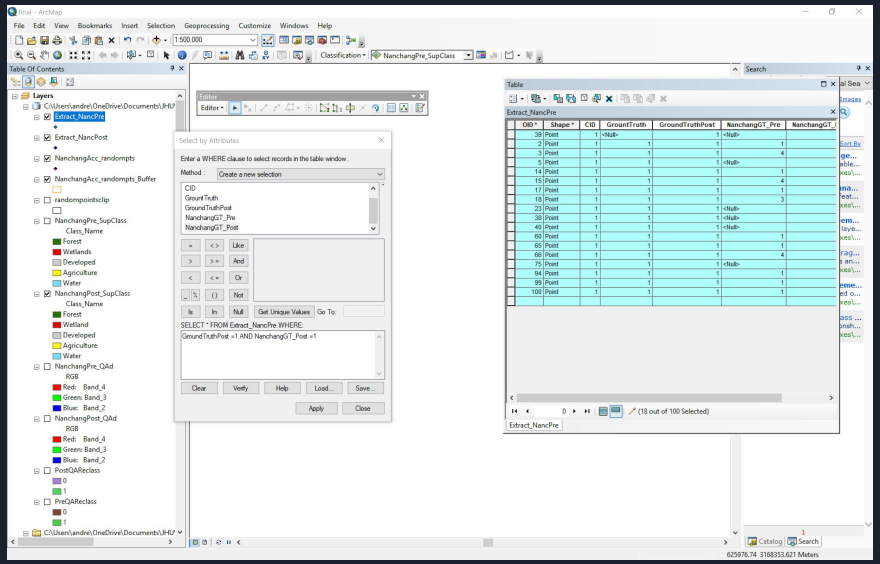

To conduct an accuracy assessment, ground truth needed to be established for sample pixels to compare with each classifier. **Left**: [Create Random Points] *and 30 m* [Buffers] *used to determine GT for 100 sample pixels.* **Right**: *Used* [Extract Values from Points] *to see classifier values for sample pixels, then compare values to populate a confusion matrix - next page.*

Accuracy Assessment Pre-Storm

Pre-Storm Classes	Forest	Wetland	Developed	Agriculture	Water	<Null>	Total	User's Accuracy
Forest	17	0	1	0	0	0	18	94%
Wetland	3	5	3	4	0	0	15	33%
Developed	2	2	12	3	0	0	19	63%
Agriculture	9	4	6	4	3	0	26	15%
Water	0	0	0	0	7	0	7	100%
<Null>	9	0	3	0	0	3	15	20%
Total	40	11	25	11	10	3	100	
Producer's Accuracy	42%	45%	48%	36%	70%	100%		

The most important class - Water performed reasonably well. In some cases water may have been misclassified as agriculture because some of the rice fields use quite a lot of water.

Accuracy Assessment Post-Storm

Post-Storm Classes	Forest	Wetland	Developed	Agriculture	Water	<Null>	Total	User's Accuracy
Forest	18	0	0	0	0	2	20	90%
Wetland	1	2	2	1	1	1	8	25%
Developed	5	1	11	2	2	1	22	50%
Agriculture	7	4	9	5	0	0	25	20%
Water	0	0	0	0	12	0	12	100%
<Null>	5	0	2	0	2	4	13	31%
Total	36	7	24	8	17	8	100	
Producer's Accuracy	50%	29%	46%	62%	70%	50%		

Again the water class performed fairly well sometimes being confused for wetland or developed. The classifiers for both pre and post storm images may have had a hard time differentiating between Developed, Agriculture, and Forest classes as rural areas were often nestled in forested mountain areas, and small farm plots were invariably located within or adjacent to developed, albeit rural, areas.

Discussion

- The classification provided satisfying results for demonstrating the dramatic change in the region resulting from the flood but would need refining to be used in analysis of how much of the population was affected, or what area of farm land (and what kind of crops) were impacted.
- For a more detailed analysis that could be used for damage assessments or demographic impacts, higher resolution imagery or radar systems might be useful. During the qualitative analysis it was hard to pin down intra-urban flooding at 30 m resolution except in the larger streams and rivers. This was unexpected considering the evidence of inundated streets in photographs in the area.
- Cloud cover was also a huge factor in both images. Because the heavy rainfall was persistent and lasted for nearly a month across China, it was impossible to find any cloud free images during and around the peak flooding. Leveraging the cloud penetrating frequencies of synthetic aperture radar systems would have been helpful for measuring flood extent during the storm.

References

Alsdorf, D., Mognard, N., Rodriguez, E. 2005. WatER: The Proposed Water Elevation Recovery Satellite Mission, AGU Fall Meeting Abstracts, Retrieved from: https://www.researchgate.net/publication/253373787_WatER_The_proposed_Water_Elevation_Recovery_satellite_mission

Bales, J.D., Wagner, C.R., Tighe, K.C., Terziotti, S. 2007. LiDAR-Derived Flood-Inundation Maps for Real-Time Flood-Mapping Applications, Tar River Basin, North Carolina, *USGS Scientific Investigations Report 2007-5032*, i-39, Retrieved from: https://pubs.usgs.gov/sir/2007/5032/pdf/SIR2007-5032.pdf

Hallegate, S., Green, C., Nicholls, R.J., Corfee-Morlot, J. 2013. Future flood losses in major coastal cities, *Nature Climate Change*, *3*, 802-806, https://doi.org/10.1038/nclimate1979

Haq, M., Akhtar, M., Muhammad, S., Paras, S., Rahmatullah, J. 2012. The Egyptian Journal of Remote Sensing and Space Sciences. Techniques of Remote Sensing and GIS for Flood Monitoring and Damage Assessment: A Case Study of Sindh Province, Pakistan, 15, 135-141.

Joyce, K., Wright, K., Ambrosia, V., Sergey, S. 2010. Incorporating remote sensing into emergency management, *Australian Institute for Disaster Resilience*, *25(4)*, Retrieved from: https://ajem.infoservices.com.au/items/AJEM-25-04-05

Mason, D.C., Giustarini, L., Garcia-Pintado, J., Cloke, H.L. 2014. International Journal of Applied Earth Observation and Geoinformation. Detection of Flooded Urban Areas in High Resolution Synthetic Aperture Radar Images Using Double Scattering, 28, 150-159. http://dx.doi.org/10.1016/j.jag.2013.12.002

Myrland, J. 2014. Two-dimensional hydraulic modeling for flood assessment of the Rio Rocha, Cochabamba, Bolivia, *Department of Earth Sciences, Uppsala University*, *i-37*, Retrieved from: http://www.w-program.nu/filer/exjobb/Johanna_Myrland.pdf

References Continued

Nirupama & Simonovic, S.P. 2002. ROLE OF REMOTE SENSING IN DISASTER MANAGEMENT, *ICLR Research*, *21*, 1-107, Retrieved from: https://ir.lib.uwo.ca/cgi/viewcontent.cgi?article=1002&context=wrrr

Poser, K., 2010, Volunteered Geographic Information for Disaster Management with Application to Rapid Flood Damage Estimation, Geomatica, 64(1), 89-98. Retrieved from: https://www.researchgate.net/publication/265619198_Volunteered_Geographic_Information_for_Disaster_Management_with_Application_to_Rapid_Flood_Damage_Estimation?enrichId=rgreq-10704ac60310e2ff04c06ef3af63e0ab-XXX&enrichSource=Y292ZXJQYWdlOzI2NTYxOTE5ODtBUzoxOTQ5NjE0NjQxMzk3ODRAMTQyMzQ5Mzg0NDAxMg%3D%3D&el=1_x_2&_esc=publicationCoverPdf

Rahman, R., Thakur, P.K., 2017. Detecting, Mapping and Analysing of Flood Water Propagation Using Synthetic Aperture Radar (SAR) Satellite Data and GIS: A Case Study from the Kendrapara District of Orissa State of India, The Egyptian Journal of Remote Sensing and Space Sciences, Forthcoming, https://doi.org/10.1016/j.ejrs.2017.10.002

Schumann, G., Bates, P.D., Horrit, M.S., Matgen, P., Pappenberger, F. 2009. Progress in integration of remote sensing-derived flood extent and stage data and hydraulic models, *Rev. Geophys., 47, RG4001*, https://doi.org/10.1029/2008RG000274

Schumann, G. 2017. Remote Sensing of Floods. *Oxford Research Encyclopedia of Natural Hazard Science*, Retrieved from: http://naturalhazardscience.oxfordre.com/view/10.1093/acrefore/9780199389407.001.0001/acrefore-9780199389407-e-265

Tamari, S., Guerrero-Meza, V. 2016. Flash Flood Monitoring With an Inclined Lidar Installed at a River Bank: Proof of Concept, Remote Sensing, 8(834), 1-10. https://doi.org/10.3390/rs8100834

Womble, J.A., Ghosh, S., Adams, B.J., Friedland, C.J., 2006. Advanced Damage Detection for Hurricane Katrina: Integrating Remote Sensing and VIEWS^{TM} Field Reconnaissance. MCEER Special Report Series, 2, i-142.